Raport Badawczy

Research Report

RB/7/2017

Spatial variability of the intake fraction from urban emission sources in Warsaw

P. Holnicki, A. Kałuszko, Z. Nahorski

Instytut Badań Systemowych
Polska Akademia Nauk

Systems Research Institute
Polish Academy of Sciences

POLSKA AKADEMIA NAUK

Instytut Badań Systemowych

ul. Newelska 6

01-447 Warszawa

tel.: (+48) (22) 3810100

fax: (+48) (22) 3810105

Kierownik Zakładu zgłaszający pracę:
Prof. dr hab. inż. Zbigniew Nahorski

Warszawa 2017

Spatial variability of the Intake Fraction from urban emission sources in Warsaw

Piotr Holnicki[1], Andrzej Kałuszko[1], Zbigniew Nahorski[1,2]

[1] *Systems Research Institute, Polish Academy of Sciences, Warsaw, Poland (holnicki@ibspan.waw.pl; kaluszko@ibspan.waw.pl; nahorski@ibspan.waw.pl)*

[3] *Warsaw School of Information Technology (WIT), Warsaw, Poland (Z.Nahorski@wit.edu.pl)*

Abstract

Increasing level of the ambient air pollution and associated adverse health effects is one of most acute environmental problems in many European cities. Air pollution dispersion models are often used to estimate population exposures and to support emission abatement strategy. The intake fraction (*iF*) approach can be applied for evaluating the health benefits of reducing emissions, especially when rapid decisions are needed. Intake fraction is a metric that represents emission-to-intake relationship and characterizes exposure potential attributed to specific emission sources. Quantification of this potential is a key information when emission abatement policy is considered. In this study, the spatial variability of *iF* in Warsaw agglomeration, Poland, is discussed. The *iF* analysis is based on the earlier air quality modeling results, that include the main pollutants characterizing an urban atmospheric environment (SO_2, NOx, PM_{10}, $PM_{2.5}$, CO, C_6H_6, B(a)P, heavy metals). The annual mean concentrations were computed by the CALPUFF modeling system (spatial resolution 0,5 x 0,5 km^2) on the basis of the emission and meteorological data from year 2012. The emission field, which is wider than the receptor area, comprises high- (power generation) and low- (industry) point sources, mobile (transport) sources and area (housing) sources. Spatial distributions of *iF*s attributed to the individual emission sources in each of the above emission categories are discussed. Moreover, the aggregated *iF* values are computed for each emission class and the related polluting compounds. The substantial increase of the respective *iF*s is shown, in both cases, when the emission field is limited to the intra-urban sources only (emission and receptor domains are identical).

Keywords:

urban air quality; pollution dispersion model; population exposure; intake fraction assessment.

1. INTRODUCTION

The intake fraction index (*iF*) represents the emission-to-exposure relationship. It is defined as the ratio of the mass of pollutant inhaled by the exposed population and the mass of pollutant emitted by a given source or by a specified category of emission sources (Levy *et al.* 2002, Marshall and Nazaroff 2006, Stevens *et al.* 2007, Tainio *at al.* 2010, Lamancusa *et al.* 2017). It depends on several factors, such as (Marshall and Nazaroff 2006) exposed population size and spatial density, distance between the source and the receptor domains, meteorological conditions controlling pollution dispersion, pollutant persistence, chemical and physical transformation (secondary pollutant formation). On the other hand, *iF* is independent of emission rate because its value is normalized, attributed to the unit emission. Intake fraction is dimensionless, recently expressed in [ppm], where 1 ppm means 1 mg inhaled for 1 kg emitted (Apte *et al.* 2012, Lamancusa *et al.* 2017). An equivalent unit [per million] – was also applied in numerous earlier studies (Bennet *et al.* 2002, Marshall and Nazaroff 2006, Stevens *et al.* 2007).

Intake fraction is an important tool in life cycle analysis and risk assessment (Bennet et al. 2002, Humbert et al. 2011) or in decision making process, when emission abatement strategy is considered (Stevens et al. 2007, Marshall and Nazaroff 2006, Marshall et al. 2005), where the population weighted intake is directly transferred to the related health effects. Given *iF*s and the emission rates for each source, optimal solutions can be searched, e.g. by the scenario or cost effectiveness analysis. It plays a similar role as *transfer matrix* of emission-to-concentration relation which is a key factor in the decision problem considered there.

In the previous studies *iF*s were assessed for different types of emission sources and pollutants. Power plant point sources (Greco et al. 2007, Zhou et al. 2003, Levy et al. 2002), domestic combustion area sources (Taimisto et al. 2011, Tainio et al. 2014) or road transport

sources (Marshall et al. 2003, 2005, Stevens et al. 2007, Apte et al. 2012, Du et al. 2012, Tainio et al. 2014, Lamancusa et al. 2017). The last group of papers usually deals with urban scale case studies where the traffic related emissions are important sources of the atmospheric environment pollution.

In this study, the intra-urban intake fraction analysis for Warsaw agglomeration is discussed, where the four basic emission categories are distinguished in the total emission field: power generating energy sources, other industrial point sources, area sources of domestic combustion, and line sources of the road transport. Analysis of iF distribution is based on the air quality modeling results for Warsaw using the emission and meteorological data for the year 2012 that are discussed in details in (Holnicki et al. 2017).

Air quality in Warsaw is mainly determined by two categories of emission sources, the domestic combustion and the traffic. These are the principal sources of particulate matter, including its fine fraction – $PM_{2.5}$, which is mainly responsible for air pollution-associated mortality (Wang et al. 2016, WHO 2016). A general situation in Poland is, that the coal combustion is the main energy source (85%), both in the industry and domestic use. In consequence, Poland is one of a few EU countries with the highest concentrations of particulate matters, including strongly carcinogenic B(a)P pollution. Coal dominates in domestic heating in the peripheral districts of Warsaw as well as in the neighboring municipal areas, while the district heating system mainly covers the central part of the city.

Road transport, due to high and steadily increasing traffic intensity in Warsaw, is another emission category influencing air quality. It contributes significantly to the total PM pollution, being at the same time the main source of NOx, CO and C_6H_6 pollutions. According to the classification applied in a global vehicle-related iF study by Apte et al. (2012), Warsaw with the total population below 2 million, situates in the category of medium

size polluted cities (subgroup EUJ). Presented below *iF* results for the mobile sources in Warsaw are matching this study general estimates.

2. METHODS

2.1 The study area and the main sources of air pollution

This study aims at estimation of the intake fractions for the main sources of air pollution in Warsaw agglomeration. The data for the analysis are taken from the air quality modeling results for Warsaw, calculated for the emission and meteorological data from the year 2012 and presented in (Holnicki *et al.* 2016, 2017)[17,20]. The annual mean concentrations are computed by CALMET/CALPUFF modeling system (Scire *et al.* 2002), with the spatial domain resolution 500m x 500m. Meteorological fields are based on the WRF model (NCAR 2008), and assimilated to the final discretization grid by the CALMET preprocessor. The air pollution results are generated as a sequence of 1-h episodes (8785 time steps) which cover the year under question. The final results comprise the annual average concentrations of the main pollutants, recorded at the fictitious receptor points.

The set of pollutants which are considered includes gaseous pollutions of SO_2, NO_X, CO, C_6H_6, particulate matter PM_{10} and $PM_{2.5}$ (including primary and re-suspended fractions as well as the sulfate and nitrate aerosols, $SO_4^{=}$, NO_3^{-}) and some heavy metals, Pb, As, Cd, Ni, as well as benso(a)pyrene B(a)P. The composition of the main polluting species, their spatial distribution and their maximum values also reflect the peculiar structure of the local emission field.

The air pollution data, together with the population density map for Warsaw agglomeration, are then used to assess the population weighted exposure (*E*) for the main polluting compounds and to compute the respective intake fraction (*iF*) estimate. This estimate can be attributed to a specified individual emission source, to a specified category of

emission sources or to the total emission field from the domain. In the sequel *iF*s are assessed for all the individual emission sources and the spatial variability of this estimate is analyzed.

2.2 The structure of the emission field and selected air quality maps

The Warsaw Metropolitan Area, about 520 km^2 within the administrative borders and total population of 1715517 inhabitants (GUS 2014, Holnicki *et al.* 2017, Warszawa 2015) is shown below in Fig. 1a. This is the receptor area, where the annual mean concentration are computed, with the homogeneous spatial resolution of 0.5 x 0.5 km.

The total emission field covers the administrative Warsaw area and the surrounding belt of approximately 30 km width, as shown in see Fig. 1b. The aggregate emission field, including the individual sources in each category, consists of 24 high point sources (energy generation), 3880 low point sources (industrial plants), 6962 area sources (residential combustion), 7285 line sources (road traffic, quantified in the grid cells). For some polluting compounds, like particulate matter, an important contribution to the resulting air pollution in Warsaw comes from the trans-boundary inflow from distant sources. This is entered in the modelling via the boundary conditions in the CALPUFF model, and is based on the EMEP modeling results.

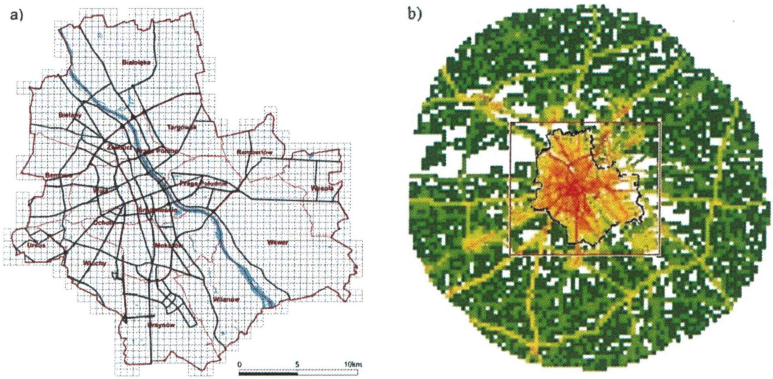

Fig. 1. The study domain: (a) discretization of the receptor area, (b) the total emission area.

The point sources are characterized by the emission parameters and location coordinates. The area and line sources are defined as grid emission squares, 0.5 km x 0.5 km inside Warsaw administrative borders (Fig. 1a), and coarser resolution (1 km x 1 km) in the surroundings (Fig. 1b). The local city areas in the suburban belt are represented by the nested fine resolution grid.

3. POPULATION WEIGHTED EXPOSURE AND THE INTAKE FRACTION

The full modeling results for Warsaw agglomeration, which are presented in Holnicki *et al.* (2017), include the concentration maps of the main compounds, and indicate the pollutants which exceed the EU limit values (CAFE 2008; EEA 2012, ME 2012) – e.g. NO_X, PM_{10}, $PM_{2.5}$ and B(a)P – in some districts of Warsaw. These results can be used to quantify the population average concentration (exposure – E) and the intake fraction (iF), attributed to a specified polluting compound and an emission source. These are closely related metrics, traditionally used by scientists and policy makers in air quality management, especially when the problem of minimizing the adverse health effect is considered. Exposure is a receptor-oriented descriptor, which quantifies the total intake (dose) of a pollutant that is inhaled by the population exposed in a given time interval. Intake fraction represents an incremental emission-to-intake relationship (sensitivity of the dose to the unit change of emission). Figure 2 presents the population density map for Warsaw (EEA 2009; GUS Report 2014), which was used to quantify the above metrics and to illustrate some basic relations between them. The spatial resolution applied in the population density map is consistent with that used in the air quality model (0.5 km x 0.5 km). The legend shows the population density as a number of inhabitants in one elementary resolution square.

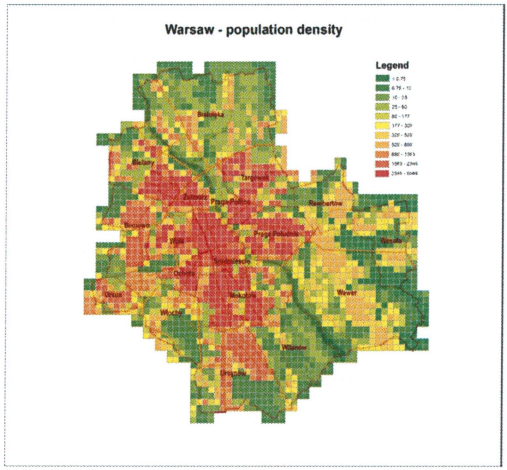

Fig. 2. Population density map for Warsaw

3.1 Exposures and the intake fractions for individual emission sources

Population weighted exposure to a selected pollutant, $E_{i,k}$ [□g/m^3], can be attributed to a specified emission source. In such a case, it quantifies an adverse environmental impact of the source and can be useful when emission reduction policy is considered. Its value can be calculated as follows:

$$E_{i,k} = \frac{1}{Pop} \sum_j C_{i,j,k} \cdot Pop_j \tag{1}$$

where $C_{i,j,k}$ is the concentration of this pollutant [□g/m^3] originating from the i-th source and measured at the j-th receptor element, Pop_j is the population of the j-th receptor element [person], Pop is the total population (1715517 assumed), i is the emission source's index within emission category, j is the receptor's index, and k is the index of the pollutant.

By definition, intake fraction is a standardized measure, calculated per unit emission, which quantifies the sensitivity of environmental impact to variation of the source's emission.

The individual *iF* (attributed to specific emission source and pollutant) can be computed according to the formula:

$$(iF)_{i,k} = \frac{BR}{Q_{i,k}} \sum_{j} C_{i,k,j} \bullet Pop_j = \frac{BR * Pop}{Q_{i,k}} * E_{i,k} \quad (2)$$

where $Q_{k,j}$ is the emission, *BR* is the breathing rate (20 m^3/day/person or ~0.00021 m^3/s/person) (Bennet *et al.* 2002, Loh *et al.* 2009, Du *et al.* 2012), and *i*, *j*, *k* as before.

Figure 3 presents intra-urban variability of the *iF* estimates attributed to the individual sources in four emission categories, depending on a specific pollutant. The box plots for the point sources (Fig. 3a) comprise all emitters within a category. In the case of the area and the mobile sources (Fig. 3b) the presented plots incorporate 2500 (aerial in both cases) emission sources with the highests *iFs*. The variability of *iF* in the high point emitters (range 0.2–4.2 ppm; IQR: 0.6–1.8 ppm) is relatively low, as these sources (24 in total) are generally homogeneous as to the emission parameters and all located inside or in the immediate vicinity of Warsaw. For the other point sources, which are about 3000 in total, the variability range is 0,1–57 ppm, with IQR 3–14 ppm, for the most basic pollutants. The only exceptions are NOx and CO, where the maximum *iF* values attributed to one emission source (#3370), with only two above mentioned components emitted, are 76.6 and 79, respectively. This source is characterized by a low stack height (7 m), very low emission rates of both pollutants and location in a densely populated, central district, which results in much higher *iF* value than for the rest of the sources. For the last two categories, with about 7000 active emission sources each, the *iF* variability for PM/CO/C_6H_6 is within the range 0–72 ppm, with IQR_{PM} 4–20 ppm for the area sources and for PM within the range 0–80 ppm, and IQR 6–30 ppm for the line sources, with the maximum of 80 ppm for the re-suspended particulate matter, PM_{10_R} and $PM_{2.5\_R}$.

When examining the Pearson correlation coefficient for the individual emitters in four emission categories, no correlation is observed between *iF*s and the related emission rates for different pollutants or sources. Due to an emission-normalized character of the *iF* metric, the impact of the emission rate on the resulting value is minor. On the other hand, the *iF* is very sensitive to the population density of the area which is affected by a specific source. This fact is illustrated by the above mentioned low point source #3370 (Fig. 3), where very low emission rate accompanied by relatively high population exposure gives higher than average *iF*.

Intra-urban variability of *iF*s attributed to individual sources also strongly depends on the emission domain that is taken into account. Figure 3 (bottom) shows the *iF* distributions, related to the area and the line sources – the categories mostly influencing urban environment – when the emission field comprises the neighborhood of Warsaw. Figure 4 shows the respective box plots, when this field is limited to the intra-urban emitters only. The highest *iF*s for the pollutants considered are the same, since they refer to the sources located inside Warsaw (compare Fig. 5 below), but the IQR's are wider and the related medians and the upper whiskers raise significantly. This increase relates to all the pollutants considered.

The next two figures compare the spatial distributions of exposure (*E*) and *iF* for the mobile sources (Fig. 5) and the area sources (Fig. 6). The plots utilize the numbering system applied in both source categories: #1–1500 are the sources in the cities surrounding Warsaw (fine grid), #1501–5500 are the sources in the rural vicinity of Warsaw (coarse grid), and over #5500 are the sources located in Warsaw (fine grid). Moreover, the distinction is marked between the sources located in the immediate outskirt of Warsaw (blue color) and those in the rural area (red color). The above outskirt is indicated by the square domain shown in Fig. 1b.

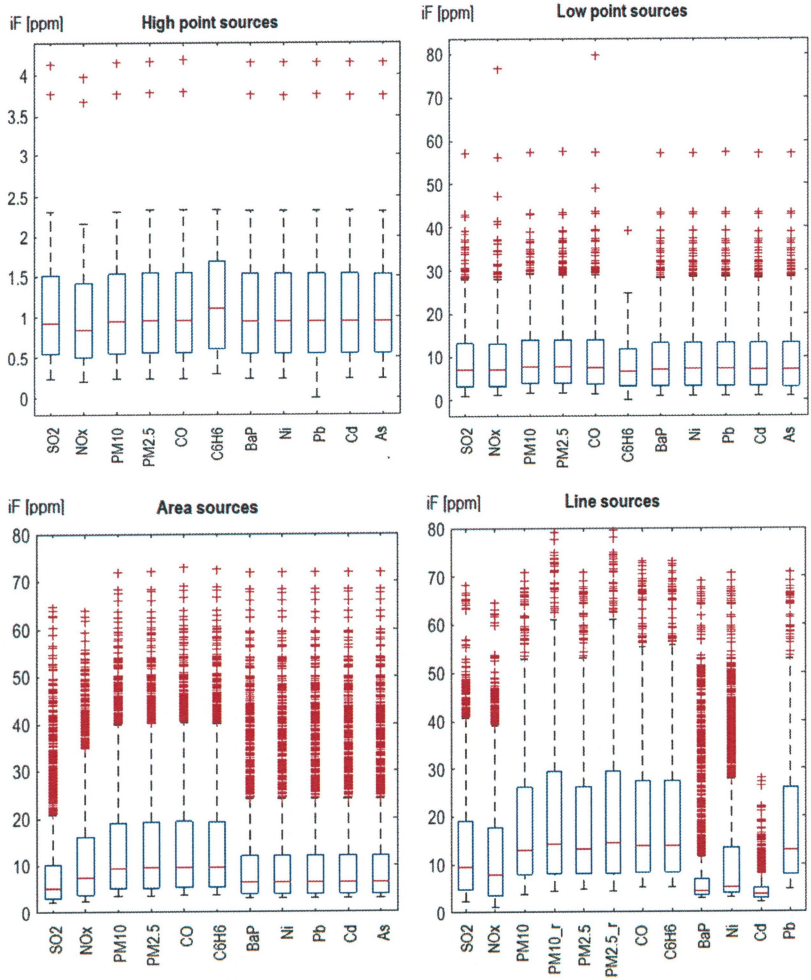

Fig. 3. Distribution of the intake fraction by source category and pollutant: the high and low point sources (top) and the area and line sources (bottom). The horizontal lines on the box indicate the 25th, 50th (median), 75th percentiles, while the whiskers show the 5th and 95th percentiles. The height of the box indicates the interquartile range (abbreviation IQR used in the text), limited by the 25th and 75th percentiles of distribution.

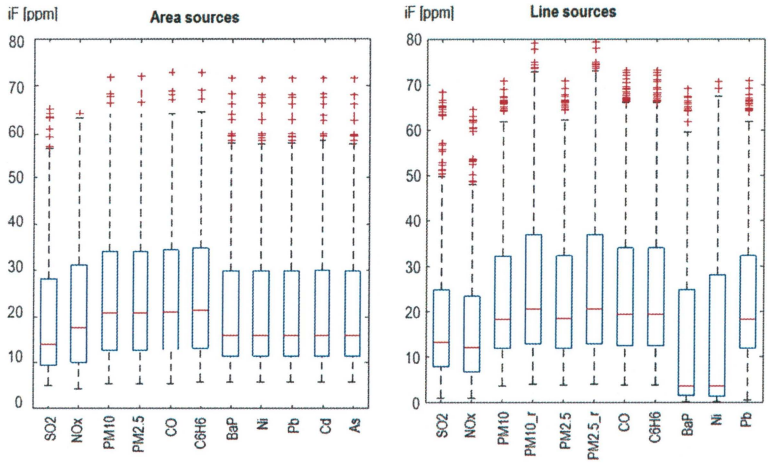

Fig. 4. Distributions of the individual *iF*s for the area (left) and the line (right) sources, when the intra-urban emission sources (only) are considered.

The spatial distributions of the *E* and *iF* estimates are similar, however there are significant differences in the variability ranges of each of them. This fact is seen in Figs. 5–6, where the model scatter plots of the exposure and intake fraction values are shown, for the selected pollutants, NOx, PM_{10} for the line sources and NOx, PM_{10} for the area sources, respectively. About 2000 dominating emission sources are considered in the plots, where the logarithmic scale of the Y-axis is applied. As stated above, all the sources in Figs. 5–6 are split down into three subgroups, according to the source location. The main difference refers to the variability range of the *E* and *iF* plots. It is above three orders of magnitude for *E* and within the range 1–60 ppm in the case of *iF*, which follows from the normalization of the last metric (2). The number of the dominating sources located in Warsaw is much higher for the mobile sources (Fig. 5). Due to the district heating system in the central part of Warsaw, most of the active area sources are located in the periphery of the city or in the city outskirt. On the other hand, Fig. 6 shows a significant contribution to *E* values of the area sources from the Warsaw outskirt, which is caused by the 4 times increase of an emission element area (1 km x 1 km).

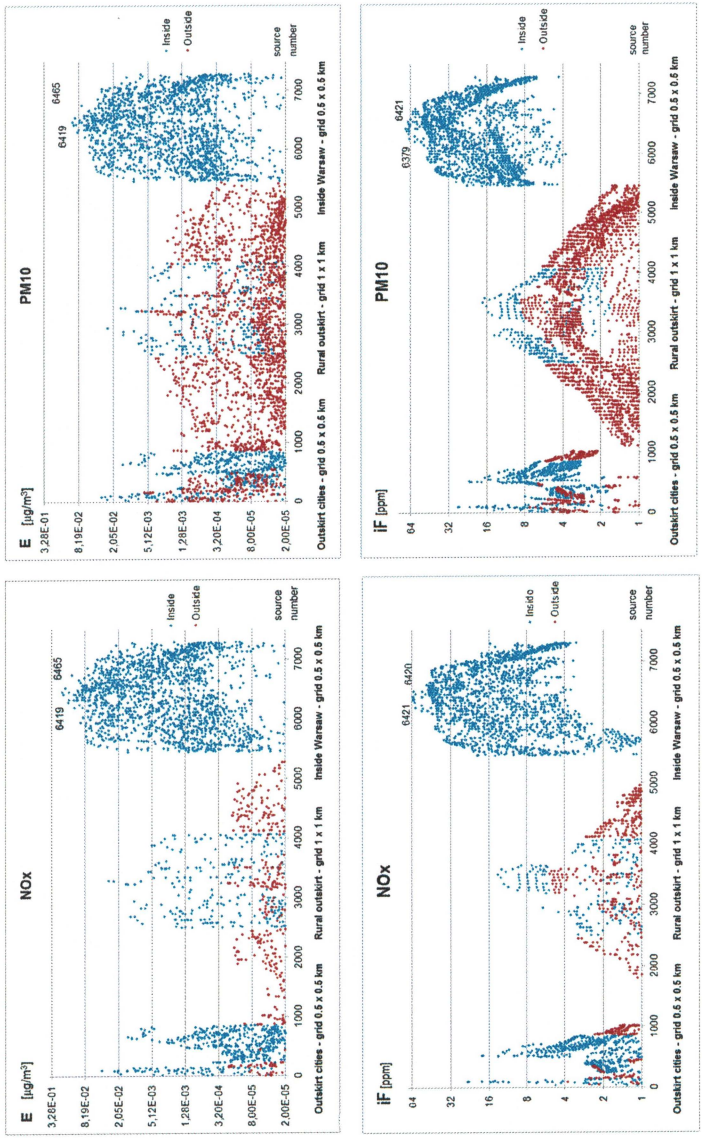

Fig. 5. Spatial distributions of the exposure (E) and (*iF*) for NOx and PM_{10} for the line sources, logarithmic scale

Fig. 6. Spatial distributions of the exposure (*E*) and (*iF*) for NOx and $PM_{2.5}$ for the area sources, logarithmic scale

Table 1. The variability ranges of exposure (E) and intake fraction (iF), and the dominating sources, depending on the pollutant and emission category

	Parameters	High Point		Low Point		Area		Line	
		E	***iF***	***E***	***iF***	***E***	***iF***	***E***	***iF***
SO_2	Variability range	5437	17,7	39084	36,5	422	22,4	988	17,1
	The dominating source	#495	#507	#2892	#566	#6084	#6433	#6465	#6421
	Second dominating source	#494	#519	#567	#805	#6121	#6495	#6419	#6379
NOx	Variability range	20288	19,1	1341	35,3	321	18,8	1163	21,1
	The dominating source	#500	#507	#2892	#566	#6084	#6433	#6465	#6421
	Second dominating source	#495	#519	#3013	#805	#6121	#6495	#6419	#6420
PM_{10}	Variability range	1298	17,5	41975	20,9	317	15,2	197	10,0
	The dominating source	#494	#507	#567	#566	#6084	#6433	#6465	#6421
	Second dominating source	#495	#519	#3085	#805	#3203	#6495	#6419	#6379

The sources attributed to the dominating exposures shown in Figs. 5–6 (top), coincide in each case with the maximum emissions. On the other hand, the highest iF values pointed out in Figs. 5–6 (bottom) never refer to the maximum emission sources. They rather reflect the other factors that determine iF, such as location, population density, etc.

The above remarks concerning the variability of E and iF metrics are also illustrated in Table 1 for selected polluting compounds in the four emission categories, where about 2000 dominating sources are considered. The variability ranges of the E and iF are calculated as the ratios E_{max}/E_{min} and iF_{max}/iF_{min}, respectively. The table shows the differences in the variability ranges of E and iF, and also confirms that the different emission sources refer to the maximum values of each of these indexes.

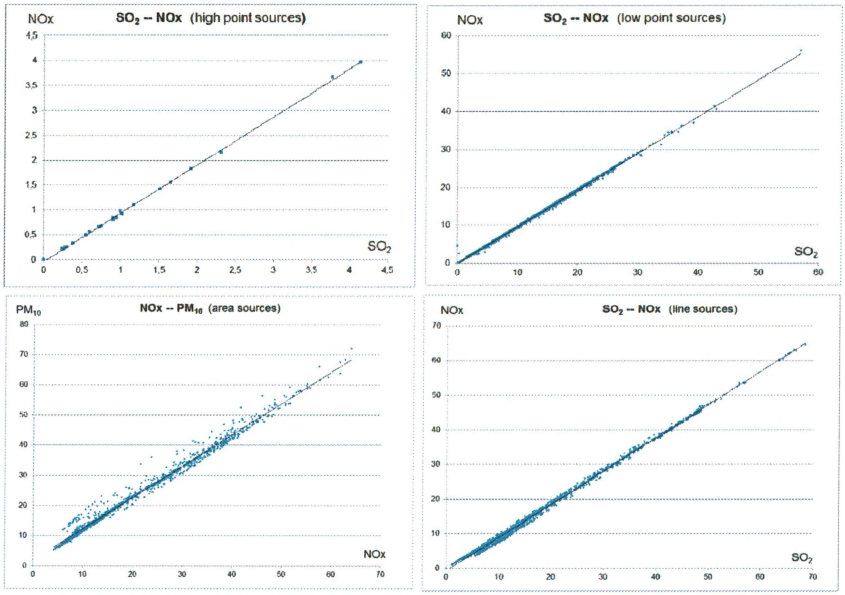

Fig. 7. Relation between the *iF*s assigned to different pollutants of the same emission source: point sources (top), area and line sources (bottom).

As stated above, *iF* does not reflect the emission rate, but other emitter's characteristics (location, technological parameters, population affected, meteorology), which are common and depend neither on the pollutant nor emission. This fact is revealed by a very high correlation between different pollutants emitted by a specified source, which is illustrated in Fig. 7. Hence, the *iF* value calculated for any selected pollutant characterizes in fact all the compounds emitted.

Generally, the emission category is also reflected in the *iF* value. As seen from Figs. 3–4 (Y-axis), the maximum values of these estimates are low for the high point sources, medium for the other point sources and the highest in the area and the line categories. Due to the high elevation of the emission points in the first category, the impact on the local

receptors is very low. On the other hand, it is significant, especially in the case of the line sources, where the emission point is at the street level.

Fig. 8 presents maps of the spatial distribution of the *iF* estimates for the area (B(a)P) and the line (NOx) emission categories, respectively. For the area sources (left panel), the maximal values occur inside the peripheral districts of Warsaw or in the immediate vicinity of the town, where the location of the area sources (mainly residential combustion, with small scale heating installations) coincides with relatively high population density. On the other hand, it is seen that the contribution of the area emission in the central part of the agglomeration is low (considerable part of the area with zero or negligible emission) due to the district heating in the main part of Warsaw.

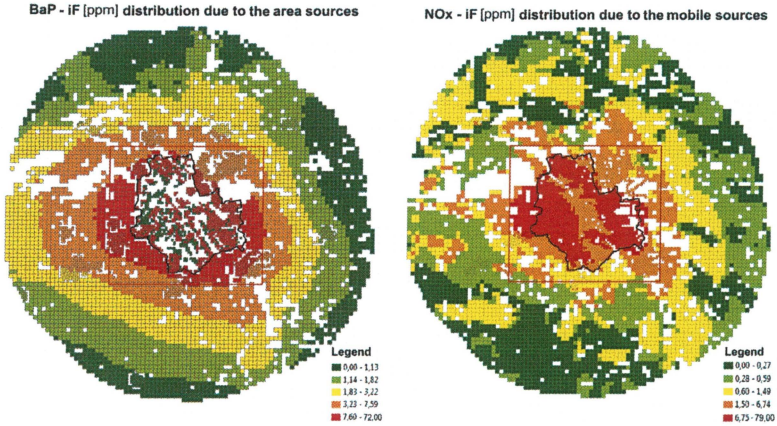

Fig. 8. Spatial distributions of the *iF*s for the area sources (left) and the line sources (right)

For the road transport sources, where *iF* distribution for NOx pollution is presented (Fig. 8, right panel), the domain of the highest *iF* related values occur inside the administrative border of Warsaw, where the high density of the street network coincides with the high population density (with the distinct decrease in value along the channel of the

Vistula), as seen from Figs. 1 and 2. The area of the dominating *iF*s connected with the mobile sources is limited and much more compact compared to that for the area sources, due to very low elevation of the emission points. This also restrains the dispersion of a pollutant and the resulting environmental impact (exposure). Analogously, the spatial *iF* distribution maps for NOx pollution in two categories of the point sources (the high point sources – left, and the low point sources – right) are presented in Fig. 9.

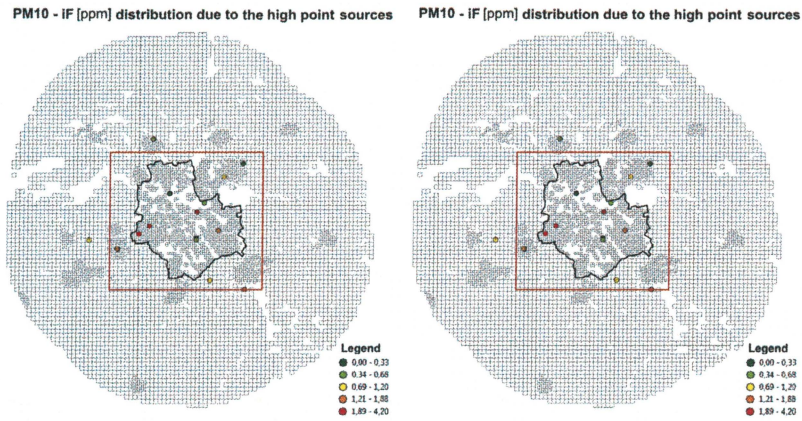

Fig. 9. The *iF* estimates for the point sources: high (left) and low (right)

For non-reactive, primary pollutants emitted by a specific emission source, the related *iF*s are very close to each other (see the relations illustrated in Fig. 7). Therefore, each *iF* demonstration map presented in Figs. 8–9 for a selected pollutant may be considered representative for other polluting compounds in the same emission category.

3.2 The intake fraction estimates aggregated for emission category

To implement an air quality plan, mainly the dominating emission categories are taken into account in calculation of the public health benefits due to emission reduction. The results presented above suggest that in the Warsaw agglomeration the area and mobile sources are

the dominating categories when the environmental impact and the risk of adverse health effects are considered. To quantify the relation between the total emission volume and the intake of a pollutant, the aggregated values of E and iF metrics for the specific emission category are used. The population average exposure that quantifies the aggregated impact of an emission category and attributed to a specified pollutant, has been calculated according to the formula:

$$E_k = \frac{1}{Pop} \sum_j Pop_j \sum_i C_{i,j,k} \tag{3}$$

where E_k is the total exposure to the selected polluting compound [μg/m^3], and the rest of the symbols is defined after equation (1).

The aggregated estimate, $(iF)_k$, for a specified pollutant can be calculated as follows:

$$(iF)_k = \frac{BR}{Q_k} \sum_j Pop_j \sum_i C_{i,j,k} = \frac{Pop \cdot BR}{Q_k} E_k \quad \text{and} \quad Q_k = \sum_i Q_{i,k} \tag{4}$$

where $(iF)_k$ is the aggregated index of the k-th pollutant attributed to emission category, Q_k is the total pollutant's emission within this category, and the rest is as in equation (2).

The exposure and the intake fractions for the secondary pollutants, $SO_4^=$ and NO_3^-, are computed as well according to (3), based on the resulting $SO_4^=$ and NO_3^- concentrations. The intake fractions of the above components are defined as the mass of the secondary pollutant inhaled per unit of the precursor emission, calculated on the basis of the atomic masses for primary (denominator) and the secondary (numerator) constituents that are taken into account in (Levy 2016, Lamancusa 2017, Tainio et al. 2014).

Table 2 presents the values of the aggregated intake fractions $(iF)_k$ and the related total emissions Q_k, computed for each emission category and all the pollutants discussed in this study. Generally, the category attributed iFs are low for the high point sources and increase successively for the low point, area and line sources, respectively. This confirms the

earlier results, presented in Section 3.2, for the individual emitters in each category. The *iF*s for the high point emissions are low, above all due to the stack height of the main power plants (50–300 m) enclosed in this category. Due to this, most of the emitted volume of pollutants is transported outside the receptor domain, which results in very low ratio exposure to emission. The ranges of the *iF* variability in both categories are rather narrow, 0.2 – 1.5 for high and 2 – 9 for low point emissions. This refers to the primary pollutants, because for the secondary particles the index is about two orders of magnitude lower. In both point emission categories all the active sources, which are located inside or in the immediate vicinity of Warsaw (see Fig. 9) are taken into consideration in calculations.

The *iF* values are greater for the area emitters (variability range of the primary pollutants,

8 – 10), and greatest in the category of the line sources (the range, 4 – 24). The total number of emitters in each of these categories is about 7000 (see section 2), but most of the distant sources have a minor impact on the receptor domain exposure. For this reason, the aggregated intake fraction computations in this case include about 2700 sources in each category, which are located inside the square domain indicated in Figs. 8–9 or in the immediate surroundings. These are the sources with the dominating contribution to environmental impact on the receptor area, responsible for 95% – 98% of the total exposure attributed to each emission category.

In the road transport category the source's emission is a segment of the streets which usually coincides with densely populated districts of the city. Moreover, in this case every emission source is at the same time the most affected receptor. As a consequence, the influence of the pollution dispersion is less evident in the case of the traffic emission.

Table 2. Emission, Q [g/s] ([mg/s] for As, Cd, Ni, BaP) and intake fraction, iF [ppm] for the main emission categories and pollutants

	High point		Low point		Area		Line		Total	
	Q	iF	Q	iF	Q	iF	Q	iF	Q	iF
SO2	358,49	**0,74**	50,94	**2,03**	142,23	**8,40**	45,24	**15,20**	596,90	**3,69**
SO4	0,00	**0,01**	0,28	**0,03**	2,97	**0,40**	0,96	**0,81**	4,21	**0,17**
NOx	256,81	**0,60**	44,78	**3,80**	86,07	**8,75**	619,98	**13,92**	1007,64	**9,60**
NO3	0,00	**0,03**	0,45	**0,18**	3,27	**0,13**	0,00	**0,60**	13,75	**0,39**
PPM10	22,74	**0,89**	21,51	**3,99**	347,59	**9,30**	52,17	**18,43**	444,00	**9,37**
PPM10_r							214,65	**22,17**	214,65	**22,17**
PPM25	7,35	**1,01**	9,65	**4,08**	272,53	**9,16**	35,21	**18,29**	324,74	**9,48**
PPM25_r							28,60	**23,97**	28,60	**23,97**
PM10	22,74	**1,19**	22,23	**4,07**	350,56	**9,35**	267,77	**22,12**	663,31	**13,83**
PM25	7,35	**1,93**	10,38	**4,26**	275,51	**9,23**	64,76	**23,65**	357,99	**11,23**
CO	61,02	**0,78**	69,35	**2,62**	263,40	**8,66**	3075,36	**24,60**	3469,12	**22,51**
C6H6	178,52	**0,57**	17,35	**2,68**	0,01	**10,09**	5,46	**13,17**	201,34	**1,09**
Pb	0,00	**1,30**	0,01	**5,39**	0,22	**9,97**	0,17	**22,79**	0,40	**14,90**
As	1,04	**1,18**	0,48	**2,80**	23,57	**9,97**			25,10	**9,06**
Cd	0,35	**0,77**	1,87	**9,08**	34,41	**9,97**	0,95	**3,69**	37,58	**9,29**
Ni	26,62	**0,86**	7,35	**5,62**	108,62	**9,96**	20,46	**16,90**	163,04	**8,86**
BaP	3,27	**1,41**	2,45	**2,31**	39,94	**8,43**	3,79	**18,19**	49,46	**8,11**

The two latter emission categories comprise a large number of sources and the aggregated *iF*s are reduced due to relatively low exposure of a significant group of emitters, which are distant from the receptor area. Results presented in Table 2 refer to the case of about 2700 sources in each category, which are located in Warsaw or in the immediate vicinity, determined by the square domain in Fig. 1b. The related *iF* values significantly increase, when the analysis is limited only to the emission sources located inside the administrative borders of the city (Fig. 1). Table 3 presents comparisons of these two cases for the area and line sources. For the line sources the intake fractions rise by the rate 1.4 – 1.7, depending on the pollutant, because about 1700 dominating sources are located inside the city. In case of Cd no increase is observed, because only 11 sources, with rather low exposure, are located inside the city. More meaningful increase rate for the area sources (2.6—2.8 times) is a result of much lower number of effective area sources (about 1000) located inside the city borders. These remarks correspond with the earlier *iF* distribution results (Fig. 4) for the individual sources in these two emission categories.

Table 3. Comparison of *iF*s depending on the emission area for the area and line categories

	SO_2	NOx	PM_{10}	PM_{25}	CO	C_6H_6	BaP	Ni	Cd	Pb
Emission	**Area sources**									
Warsaw + vicinity	8,40	8,75	9,35	9,23	8,66	10,09	8,43	9,96	9,97	9,97
Warsaw only	23,45	23,59	24,74	24,47	23,66	26,02	23,13	25,87	25,88	25,88
Emission	**Line sources**									
Warsaw + vicinity	15,20	13,92	22,12	23,65	24,60	24,52	13,17	16,90	3,69	22,79
Warsaw only	25,96	24,40	36,94	38,80	34,70	34,67	21,34	26,93	3,28	33,02

4. SUMMARY & DISCUSSION

The study presents a multi-species analysis of the intra-urban variability of the intake fraction, related to the emission field affecting the Warsaw Metropolitan Area. Computations are based on the modeling results for the year 2012 (Holnicki *et al.* 2017), combined with the population density data for Warsaw (EEA 2009, GUS Report 2014). The set of pollutants contains the main species characteristic for urban agglomerations: particulate matter, sulfur- and nitrogen oxides, carbon monoxide, benzene, some heavy metals and benzo(a)pyrene. Emission data available comprises a much wider area than the administrative domain of Warsaw, assumed to be the receptor domain. All the emission sources are divided into four categories, depending on the basic emission parameters: high point sources (energy sector), other point sources (industry), area sources (residential heating), line sources (road transport).

An analysis of the intra-urban *iF* variability of the individual emission sources, for the emission field that includes emitters in the immediate outskirt of Warsaw, is presented in Subsection 3.1. Box plots of the statistical *iF* distributions (Fig. 3) in four emission categories show the low values for the point sources (maximum, median, IQR), and higher for the area and line sources. The distributions are similar (independent of the pollutant) in the case of point sources, and more differentiated for the area and line sources. A significant increase of the main metrics occurs when the emission field is limited to the area of Warsaw (Fig. 4) due to increased scaling parameter (reverse of emission magnitude). Spatial distributions of *iF* and *E* estimates for the last two categories are compared in Figs. 5-6. Dominating *iF*s are attributed to sources located inside the city, but the share of the sources in the immediate outskirt is substantial. The variability range of *iF*, which is normalized, is low compared with the variability of *E*. Relatively high exposures of some area sources in the outskirt of Warsaw results from the larger area (1 km^2) of an elementary emitter.

In general, the most important factors influencing the intake fraction are, as stated above, source location (distance from the receptor domain in our case), density and size of the population exposed, meteorological conditions, pollutant persistence and transformations. The elevation of the effective emission point is another important factor, see Fig. 3, Table 2, and Table 3. As a rule, *iF* values (mean, maximum, IQR) rise for high- , low-point, area and line sources, respectively. Emission rate, which appears in the denominator of the expression in equation (2), has no impact on *iF*. Strong correlation is observed between *iF*s of the primary pollutants emitted by a specified source (selected examples shown in Fig. 7). On the other hand, similar or identical sources with different locations can substantially differ in *iF* values, due to a strong impact of the spatially variable population density.

Spatial distributions of *iF*s attributed to the individual sources in four emission categories, illustrated on maps in Figs. 8-9, are quite characteristic for the area and the line emitters. The highest *iF*s of the area category are connected with the sources located in the peripheral districts of Warsaw or in the close neighborhood (domestic heating). Very low (or zero) values in the central part of the city are the consequence of the district heating there. On the other hand, the domain of the highest *iF*s for the line sources is compact, more limited, and covers the central districts, where high population density coincides with high traffic intensity. The demonstration maps in Fig. 8 refer to BaP (area sources) and NOx (line sources), respectively. However, the maps are representative for any pollutant within the same emission category, and the respective maps for the other pollutants throughout emission class are almost identical. This is an effect of high correlation between the pollutants emitted by an individual source. The minor differences, if any, follow from the fact that some specified sources can differ in terms of emitted pollutants composition. Hence, a representative *iF* estimate for one pollutant can be sufficient for quick inspection.

Table 2, which presents the aggregated *iF*s for each emission category, confirms the dominating impact of the domestic heating and the road transport., which mainly results from low elevation of the effective emission point. Furthermore, the relation between the emission and receptor areas (Table 3) illustrates a significant increase of the aggregated *iF* estimates, especially for the area sources, when the emission field is limited to the Warsaw area, as a large group of sources located in the outskirt of Warsaw with relatively low exposure/emission ratio, are cut-off. These results correspond with the similar effect observed for the individual sources (Fig. 3), or suggested by the spatial *iF* distributions (Fig. 8).

The results of the present study are compared in Table 4 with several earlier *iF* estimates. The previous results differ in the spatial scale of the region, method of analysis, basic emission category and pollutants analyzed. Thus, we mainly refer to the papers that address the urban scale case studies, spatially distributed emission fields (mainly the mobile sources) and the related polluting factors. For comparison we use the aggregated *iF*s from the present study, estimated for the emission domain consistent with the administrative border of Warsaw (Table 3).

In Tainio *et al.* (2014) study also the CALPUFF model is used to estimate *iF*s for distributed and point sources in Warsaw agglomeration, using the spatial resolution 1 x 1 km^2 and the input data for the year 2005. Their results are compatible with the present study estimates and are only slightly higher for the area sources and slightly lower for the mobile ones. In (Apte et al. 2012) one-compartment method is applied for global analysis of ground-level emissions in 3646 cities, of the total population of 2 billion. Their mean *iF* values for the conserved primary pollutants are comparable with those from the present study. Humbert et al. (2011) analyze the primary and secondary, ground-level emissions of $PM_{2.5}$ in an urban area, on the basis of expert opinions. Results are comparable with the traffic related *iF*s in this study.

Table 4. Comparison of the obtained intake fraction estimates (in ppm) with the earlier studies.

Reference	Region/pollution	Method	Reference *iF*	This study *iF*
Tainio et al. (2014)	Warsaw urban area, domestic and traffic emissions (year 2005, resolution 1 x 1 km^2)	CALPUFF model	a t PM_{10} 21 45 $PM_{2.5}$ 20 44 NOx 18 30 SO_2 18 32	a t PM_{10} 25 37 $PM_{2.5}$ 24 39 NOx 24 24 SO_2 23 26
Apte et al. (2012)	Urban area - conserved pollutants from ground level emission	Global summary – one compartment method	am – 39 gm – 26	a t PM 25 39 CO 24 35 C_6H_6 26 35
Humbert et al. (2011)	Urban area – primary and secondary $PM_{2.5}$ (ground-level emissions)	Expert group analysis	a / t $PM_{2.5}$ 44 SO_4 0.89 NO_3 0.18	a t $PM_{2.5}$ 25 39 SO_4 0.40 0.81 NO_3 0.13 0.60
Marshall et al. (2003)	Urban area (South Coast Air Basin, US) – traffic emissions of carbon monoxide and benzene	Monitoring data combined with time-activity patterns	t CO 32 C_6H_6 33	a t CO - 35 C_6H_6 - 35
Marshall et al. (2005)	Urban area – traffic emissions	One compartment method	21	a t PM - 39 CO - 35 C_6H_6 - 35
Stevens et al. (2007)	Mexico City – ground level primary $PM_{2.5}$	Five different methods compared	26 – 120	$PM_{2.5}$ -- 39
Loh et al. (2009)	Helsinki area- benzene from vehicles	EXPOLIS data	C_6H_6 39	C_6H_6 35
Taimisto et al. (2011)	Urban area (Finland) -- traffic, primary $PM_{2.5}$	Urban Dispersion Modeling system, FMI	$PM_{2.5}$ 9.7	$PM_{2.5}$ 39
Greco et al. (2007).	Particular matter $PM_{2.5}$ primary/secondary across the US	Dispersion model -- the mobile emissions in urban areas	t $PM_{2.5}$ 9.8 SO_4 1.7 NO_3 0.23	a t $PM_{2.5}$ - 39 SO_4 - 0.81 NO_3 - 0.60

Abbreviations: a – area sources, t – traffic sources, am – arithmetic mean, gm – geometric mean.

Estimates obtained by Marshall et al. (2003) for CO and C_6H_6 from traffic emissions in South Coast Air Basin in US (calculated for monitoring data combined with time-activity patterns) are also close to the respective *iF*s in this study. In Marshall et al. (2005) the mean *iF* for urban traffic emissions (21 ppm) obtained by one-compartment model is lower than the

present study estimates, but they apply lower breathing rate (12.2 m^3d^{-1}). Updating their *iF* value with our breathing rate of 20 m^3d^{-1} very close value of 34.4 is obtained. Stevens et al. (2007) compare five methods to estimate *iF* for $PM_{2.5}$ in Mexico City. The resulting values range from 26 ppm (regression) up to 120 ppm (steady state box model) versus our 39 ppm. However, it must be noted that Mexico City, as classified in (Apte et al. 2012), is a megacity with several million inhabitants and high population density, much different from the Warsaw conditions. Intake fraction estimate by Loh et al. (2009) for benzene emitted by vehicles in the Helsinki urban area (39 ppm) is very close to our result for the line sources (35 ppm). On the other hand, an aggregated results for $PM_{2.5}$ urban emissions in Finland (Taimisto *et al.* 2011) are lower than the respective estimates in this study. One of the possible reasons is the lower population size and density in agglomerations in Finland, another one – very high re-suspended PM emission in Warsaw due to intensive traffic (Holnicki *et al.*. 2017). Greco et al. (2007) apply dispersion model to analyze primary and secondary $PM_{2.5}$ emissions in urban areas (US). The resulting *iF*s in this study are the averaged from 19 agglomerations, and the estimate for the primary $PM_{2.5}$ is similar to that from Taimisto *et al.* (2011) that may be also due to comparable traffic conditions in both cases.

RFERENCES

Apte, J.S., Bombrun, E., D. Marshall, J.D., Nazaroff, W.W. (2012). Global Intraurban Intake Fractions for Primary Air Pollutants from Vehicles and Other Distributed Sources (2012). Environmental Science & Technology, 46, 3415-3423.

Bennet, D.H., McKone, T.E., Evans, J.S., Nazaroff, W.W., Margni, M.D., Jolliet, O., Smith, K.R. Defining Intake Fraction (2002a). Environmental Science and Technology, 49, May 1, 206A-211A.

Bennet, D.H., Margini, M.D., McKone, T.E., Jolliet, O. (2002b). Intake Fraction for Multimedia Pollutants: A Tool for Life Ctcle Analysis and Coparative Risk Assessment. Risk Analysis, 2, 905-918.

CAFE (2008). Directive 2008/50/EC of the European Parliament and of the Council of 21 May 2008 on ambient air quality and cleaner air for Europe.

Du, X., YeWu, Y., Fu, L., Wang, S., Zhang, S., Hao, J. (2012). Intake fraction of PM2.5 and NOx from vehicle emissions in Beijing based on personal exposure data. Atmospheric Environment, 57, 233-- 243.

EEA (2009) (European Environment Agency); http://www.eea.europa.eu/data-and-maps/data-population-density-disaggregated-with-corine-land-cover-2000-1

EEA (2012). European Environment Agency. Air quality in Europe – Report No 4/ 2012.

ETC/ACM (2013). Technical Paper 2013/11 (R. Rouil, B. Bessagnet, eds). How to start with PM modelling for air quality assessment and planning relevant to AQD.

Greco, S.L., Wilson, A.M., Spengler, J.D., Levy, J.I. (2007). Spatial patterns of mobile source particulate matter emissions-to-exposure relationships across the United States. Atmospheric Environment, 41, 1011–1025

GUS Report 2014. Powierzchnia i ludność w przekroju terytorialnym w 2014 r. In: Główny Urząd Statystyczny [on-line]. 2014. http://stat.gov.pl/obszary-tematyczne/ludnosc/ludnosc/powierzchnia -i-ludnosc-w-przekroju-terytorialnym-w-2014-r-,7,11.html

Holnicki, P., Kałuszko, A., Nahorski, Z., Stankiewicz, K., Trapp, W. (2017). Air quality modeling for Warsaw agglomeration. Archives of Environmental Protection, 43, 1, 48-64.

Holnicki, P., Kałuszko, A., Trapp, W. (2016), The urban scale application and validation of the CALPUFF model. Atmospheric Pollution Research, 7, 393 - 402.

Holnicki, P., Nahorski, Z (2015). Emission Data Uncertainty in Urban Air Quality Modeling – Case Study. Environmental Modeling & Assessment, 2, 583 – 597.

Humbert, S., Marshall, J.D., Shaked, S., Spadaro, J.V., Nishioka, Y., Preiss, P., McKone, T.E., Horvath, A., Jolliet, O. (2011). Intake Fraction for Particulate Matter: Recommendations for Life Cycle Impact Assessment. Environmental Science & Technology, 45, 4808-4816.

Lamancusa, C., Parvez, F., Wagstrom, L. (2017). Spatially Resolved intake fraction estimates for primary and secondary particulate matter in the United States. Atmospheric Environment, 150, 229–237.

Levy, J.I. (2016). Fine Particulate Matter Assessment. and Risk Management. Risk Analysis, DOI:10.1111/risa.12673.

Levy, J.I., Wolff, S.K., Evans, J.S. (2002). A Regression-Based Approach for Estimating Primary and Secondary Particulate matter Intake Fractions. Risk Analysis, 22, 5, 895-904

Loh, M.M., Soares, J., Karppinen, A., Kukkonen, J., Kangas, L., Riikonen, K., Kousa, A., Asikainen, A., Jantunen, M.J. (2009). Intake fraction distributions for benzene from vehicles in the Helsinki metropolitan area. Atmospheric Environment, 43, 301 -- 310.

Marshall, J.D., Riley, W.J., McKone, T.E., Nazaroff, W.W. (2003). Intake fraction of primary pollutants: motor vehicle emissions in the South Coast Air Basin. Atmospheric Environment,
37, 3455-3468.

Marshall, J.D., Soon-Kay, T., Nazaroff, W.W. (2005). Intake fraction of nonreactive vehicle emissions in US urban areas. Atmospheric Environment, 39, 1363-1371.

Marshall, J.D., Nazaroff, W.W. (2006). https://depts.washington.edu/airqual/reports/10 Intake Fraction, 237-251.

ME (2012). Ministry of the Environment. Decree 1031, 24 Aug. 2012, On the admissible levels of some substances in the air (in Polish).

NCAR (2008). A description of the advanced research WRF Version 3. NCAR Technical Note,
TN–475+STR. Boulder, Colorado, USA June 2008.

Scire, J.S., Strimaitis, D.G., Yamartino, R.J. (2000). A User's Guide for the CALPUFF Dispersion Model. Earth Technology Inc.

Stevens, G., de Foy, B., West, J.J., Levy, J.I. (2007). Developing intake fraction estimates with limited data: Comparison of methods in Mexico City. Atmospheric Environment, 41, 3672-3683.

Taimisto, P., Tainio, M., Karvosenoja, N., Kupiainen, K., Porvari, P., Karppinen, A., Kangas, L., Kukkonen, J., Tuomisto, J.T. (2011). Evaluation of intake fractions for different subpopulations due to primary fine particulate matter (PM2.5) emitted from domestic wood combustion and traffic in Finland. Air Quality Atmosphere & Health, 4, 199-209.

Tainio M. (2015). Burden of disease caused by local transport in Warsaw, Poland. Journal of Transport & Health, 2(3), 423-433.

Tainio, M., Holnicki, P., Loh, M.M., Nahorski, Z. (2014). Intake Fraction Variability Between Air Pollution Emission Sources Inside an Urban Area. Risk Analysis, 34, 2021-2034.

Tainio M., Kukkonen J., Nahorski Z. (2010). Impact of airborne particulate matter on human health: An assessment framework to estimate exposure and adverse health effects in Poland. Archives of Environmental Protection, 36(1), 95-115.

Warszawa (2015). https://pl.wikipedia.org/wiki/Warszawa

Wang, T., Jerrett, M., Sinsheimer, P., Zhu, Y. (2016). Estimating PM2.5-associated mortality increase in California due to the Volkswagen emission control defeat device. Atmospheric Environment, 144, 168–174.

WHO Report (2016) "Air pollution levels rising in many of the world's poorest cities". http://www.who.int/mediacentre/news/releases/2016/air-pollution-rising/en/

Zhou, Y., Levy, J.I., Hammitt, J.K., Evans, J.S. (2003). Estimating population exposure to power plant emissions using CALPUFF: a case study in Beijing, China. Atmospheric Environment, 17, 815-826.